AIMS Biophysics, 5(4): 290–302.
DOI: 10.3934/biophy.2018.4.290
Received: 17 October 2018
Accepted: 13 December 2018
Published: 17 December 2018

http://www.aimspress.com/journal/biophysics

Research article

Functional characterizations of polyethylene terephthalate-degrading cutinase-like enzyme Cut190 mutants using bis(2-hydroxyethyl) terephthalate as the model substrate

Yoshiji Hantani[1], Hiroshi Imamura[2], Tsubasa Yamamoto[2], Akane Senga[1], Yuri Yamagami[1], Minoru Kato[2], Fusako Kawai[3] and Masayuki Oda[1,*]

[1] Graduate School of Life and Environmental Sciences, Kyoto Prefectural University, 1-5 Hangi-cho, Shimogamo, Sakyo-ku, Kyoto, Kyoto 606-8522, Japan
[2] College of Life Sciences, Ritsumeikan University, 1-1-1 Noji-higashi, Kusatsu, Shiga 525-8577, Japan
[3] Center for Fiber and Textile Science, Kyoto Institute of Technology, Matsugasaki, Sakyo-ku, Kyoto, Kyoto 606-8585, Japan

* **Correspondence:** Email: oda@kpu.ac.jp; Tel: +81757035673; Fax: +81757035673.

Abstract: A mutant of cutinase-like enzyme from *Saccharomonospora viridis* AHK190, Cut190_S226P/R228S, designated as Cut190*, possesses high-thermal stability and has high polyethylene terephthalate (PET)-degrading activity. The functional characterizations of PET-degrading enzymes are generally conducted using accessible substrates such as poly(butylene succinate-*co*-adipate) (PBSA) and *p*-nitrophenyl butyrate (pNPB), even though their structures are different from that of PET. Bis(2-hydroxyethyl) terephthalate (BHET) is a component of PET, and the structure is similar to that of PET compared to PBSA and pNPB. Therefore, the analysis using BHET as the substrate is important to evaluate effective PET degradation. In this study, we analyzed the enzymatic activity of Cut190* using BHET under various conditions including Ca^{2+} concentration and pressure. Although terephthalate was supposed to be the final product, the intermediate product, mono(2-hydroxyethyl) terephthalate (MHET), was the only product generated, possibly due to the low binding affinity of MHET. The Cut190* activity towards BHET was observed even in the absence of Ca^{2+} and increased with increasing Ca^{2+} concentration, which is similar to its activity towards pNPB, but different from its activity towards PBSA. The difference can be attributed to the size of substrates. We also analyzed the activities of Cut190* and another

high-activity mutant, Cut190*Q138A/D250C-E296C, under high pressures up to 400 MPa. BHET was non-enzymatically hydrolyzed under high pressure at 37 ℃. Enzyme activities were maintained under high pressures, and degradation of BHET in the presence of enzyme was higher than that in the absence of enzyme. Furthermore, the structural analysis of Cut190* under high pressure using Fourier transform infrared spectroscopy showed that most of the enzyme molecules were populated in the native structure below 400 MPa. These results indicate that BHET can contribute to the effective functional analysis of PET-degrading enzyme, and the combination of enzyme and pressure can lead to eco-friendly PET degradation.

Keywords: Ca^{2+}-dependent enzyme activity; high-activity mutant; high pressure; polyethylene terephthalate degradation; protein structure-activity relationship

Abbreviations: PET: polyethylene terephthalate; Cut190: a cutinase-like enzyme from *Saccharomonospora viridis* AHK190; Cut190*: Cut190_S226P/R228S mutant; PBSA: poly(butylene succinate-*co*-adipate); pNPB: *p*-nitrophenyl butyrate; BHET: bis(2-hydroxyethyl) terephthalate; TPA: terephthalate; MHET: mono(2-hydroxyethyl) terephthalate; FTIR: Fourier transform infrared; DMSO: dimethyl sulfoxide

1. Introduction

Polyethylene terephthalate (PET) has been widely used in our everyday lives, as it possesses great strength, stiffness, ductility, transparency, and lightness. As PET is practically non-degradable, post-consumer PET is a major cause of environmental concern. Chemical recyclings involving glycolysis, hydrolysis, and aminolysis are some of the potential treatments, but they generally require high temperatures and often generate additional environmental pollutants. Enzymatic methods are being investigated, as they are less energy consuming and environmentally friendly; several PET-degrading enzymes have also been reported [1,2]. However, most of the enzymes can only degrade the surface morphology. Significant decay of the polymer structure, especially the inner block leading to significant weight loss, is only detected at temperatures higher than the glass transition temperature of PET, which is between 60–65 ℃ in aqueous solutions [3–5]. Therefore, there is a need to develop enzymes with higher degradation activity and thermal stability, as well as eco-friendly chemical PET-degrading methods for industrial applications.

We have structurally and functionally characterized Cut190, a cutinase-like enzyme from *Saccharomonospora viridis* AHK190, and also obtained its mutants with higher degradation activity and thermal stability [4–9]. A unique feature of Cut190 is that its function and stability are regulated by Ca^{2+} binding [4–8]. The mutant, Cut190_S226P/R228S (Cut190*), has higher activity and thermal stability than the wild-type of Cut190 [4]. We used Cut190* as the template to obtain mutants with high activity, and successfully obtained the mutant, Cut190*Q138A/D250C-E296C, which exhibited the degradation rate of 26.6% towards amorphous PET (PET-GF) films [5].

The functional analysis of PET-degrading enzymes is generally performed using substrates such as poly(butylene succinate-*co*-adipate) (PBSA) and *p*-nitrophenyl butyrate (pNPB), although their structures are different from that of PET. Bis(2-hydroxyethyl) terephthalate (BHET) is produced as

an intermediate of enzymatic degradation of PET, and the structure of BHET is similar to that of PET compared to PBSA and pNPB (Figure S1). In addition, BHET has two sites cleaved by PET-degrading enzyme, the products (terephthalate (TPA) and mono(2-hydroxyethyl) terephthalate (MHET)) can be easily quantified by HPLC. Therefore, the analysis using BHET as a substrate is meaningful to effectively evaluate PET degradation.

In this study, we analyzed the effects of Ca^{2+}, substrate, and enzyme concentrations on the enzymatic activity of Cut190* on BHET under various conditions including pH and temperature to find the optimum condition, and compared them with the results for PBSA and pNPB reported previously [4]. We also analyzed the effect of pressure on the enzyme activity. Enzyme activity enhancement by high pressure has been reported [10–13]. Quartinello et al. recently reported that pressure of 4 MPa along with a high temperature of 250 ℃ enhanced PET degradation non-enzymatically [14]. We therefore expected synergistic effects of enzyme activity under high pressure and analyzed the effects of pressure on BHET hydrolysis by enzymes, Cut190* and Cut190*Q138A/D250C-E296C, whose degradation rates towards amorphous PET films were quantitatively evaluated [4,5]. We further analyzed the structural stability of Cut190* under high pressure using Fourier transform infrared (FTIR) measurements.

2. Materials and methods

2.1. Materials

TPA and BHET were purchased from Sigma-Aldrich Japan K.K. (Tokyo, Japan) and Tokyo Chemical Industry Co., Ltd. (Tokyo, Japan), respectively. MHET was synthesized, as described previously [5,15]. Acetonitrile (HPLC grade) was purchased from Kanto Chemical Co., INC. (Tokyo, Japan). The enzymes, Cut190* and Cut190*Q138A/D250C-E296C, were overexpressed in *Escherichia coli*, and purified as described previously [5].

2.2. Enzyme activity analysis

For enzyme activity assays, the model substrate of PET, BHET, was used. Because of low solubility, BHET was dissolved in dimethyl sulfoxide (DMSO). The assays were carried out in 50 mM Tris-HCl (pH 7.5) containing 1% (v/v) DMSO, 5 mM $CaCl_2$, and 1 mM BHET, which was slightly modified for the purpose of respective experiments. Reactions were initiated by addition of the enzyme (final concentration, 1 μM). Assays except high-pressure experiments were performed in a final volume of 75 μL, and incubated at 37 ℃ for 2 h. The reaction was stopped by the addition of 75 μL of 1% (v/v) trifluoroacetic acid. Products were analyzed using HPLC as described below.

Products were monitored at a wavelength of 254 nm on an Agilent 1200 series HPLC (Agilent technologies, USA). Sample (5 μL) was loaded onto a reversed phase column RP-C18 (Agilent ZORBAX Eclipse Plus C18 (particle size, 1.8 μm; pore size 95 Å; length, 50 mm; inside diameter, 2.1 mm)) and eluted using a mobile phase (acetonitrile/water/formic acid (15/85/0.1, v/v/v)) at a flow rate of 0.6 mL min^{-1}. The amounts of MHET and TPA produced in the reaction mixture were calculated from respective standard curves.

2.3. Enzyme activity analysis under high pressure

High-pressure experiments were performed using high-pressure hand pump and 25 mL high-pressure reactor (Syn Corporation Ltd, Kyoto, Japan) under the condition as follows: 1 μM enzyme and 1 mM BHET in 50 mM Tris-HCl (pH 7.5) containing 1% (v/v) DMSO and 5 or 25 mM $CaCl_2$ were loaded into Tygon tube (Tygon®2375, Saint-Gobain Performance Plastics, Tokyo, Japan) and pressurized to keep at 50, 100, 200, 300 and 400 MPa, respectively, at 37 ℃ for 2.5 h. After 2.5 h, reactors were decompressed. Non-pressure treated samples were also examined as a controlled experiment. Trifluoroacetic acid (1% (v/v), 50 μL) was added to 50 μL of the reaction mixtures to stop the enzyme reaction, and the product was analyzed using HPLC as described above.

2.4. Structural analysis under high pressure

FTIR measurement was used to monitor secondary structures of proteins under high pressure [16,17]. The solution of 0.29 mM Cut190* in 50 mM Tris-DCl with pD of 8.5 (adding 0.4 to the pH meter reading) was loaded into a diamond anvil cell with a gasket with a thickness of 100 μm. Barium sulfate was added to the sample as an internal pressure calibrant [18]. The cell was connected to a circulating water bath to control the sample temperature at 23.6 ± 0.1 ℃. IR spectra were recorded on a FTIR spectrometer (Jasco FT/IR-6600) equipped with a MCT liquid nitrogen-cooled detector. Prior to measurement, pressure was applied to the sample at the average rate of ~0.2 GPa h^{-1} (up to 1.2 GPa) for ~6 h to complete hydrogen-deuterium exchange of the amide protons, which was confirmed by monitoring the intensity of the amide II band. To obtain a spectrum with a resolution of 2 cm^{-1}, 512 interferograms were collected. Spectral analyses were performed using GRAMS Research for System2000 FTIR version 3.01B (Galactic Software) and IGOR Pro version 6.22A (WaveMetrics, Portland, OR).

3. Results

3.1. Hydrolysis of BHET

Enzymatic hydrolysis of BHET was evaluated monitoring hydrolysis products by reversed-phase HPLC. TPA and MHET were identified based on references molecules (Figure S2). The time taken by Cut190* to hydrolyze BHET was investigated (Figure S3). Although TPA was supposed to be the final product (Figure S1) [5], MHET was the only product generated after 24 h of reaction. The hydrolysis of BHET was also observed in the absence of Cut190*, and the amount of MHET increased in a time-dependent manner. Therefore, we determined the MHET amount generated in assays both with and without the enzyme in the following experiments.

3.2. Effect of DMSO on BHET hydrolysis

Due to the low solubility of BHET, DMSO was used as the solvent. Hence, the effects of DMSO on BHET hydrolysis by Cut190* were analyzed (Figure S4). The results showed that the enzyme activity decreased as DMSO concentration increased. Based on the results, DMSO concentration was fixed at 1% in the following experiments.

3.3. Effect of Ca^{2+}, substrate, and enzyme concentrations on BHET hydrolysis

Effects of Ca^{2+}, substrate, and enzyme concentrations on Cut190* activity towards BHET were investigated. The enzyme activity was observed even in the absence of Ca^{2+} and increased in a Ca^{2+} concentration-dependent manner up to 25 mM (Figure 1A). There was little difference in the amount of product when $CaCl_2$ concentration was between 25 and 125 mM. The concentration of Ca^{2+} used in the following experiments was 5 mM or 25 mM, which was used in the previous studies on activities of Cut190 and its mutants towards PBSA or pNPB [4]. These concentrations were selected so that we could compare our results with the Cut190* activity towards PBSA and pNPB reported previously [4].

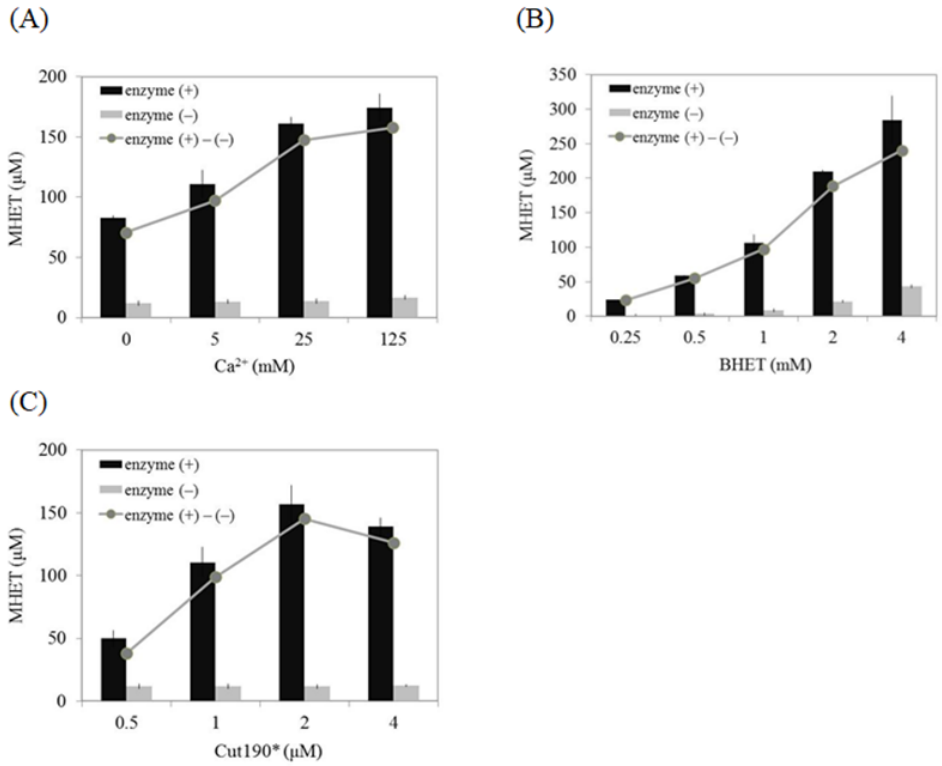

Figure 1. Effect of Ca^{2+} (A), substrate (B), and enzyme (C) concentrations on Cut190* activity towards BHET. Black and grey bars were MHET amounts in the reaction mixtures with and without enzyme, respectively. Grey circles were MHET amounts subtracted without enzyme from with enzyme to indicate net enzyme activities. Data are shown with the standard deviation of triplicate measurements.

Product amount increased as the substrate concentration increased (Figure 1B). Because substrate concentration above 4 mM could not be used due to low solubility, we could not detect the maximum velocity (V_{max}). Therefore, we could not determine the Michaelis constant (K_m) of BHET. Substrate concentration above 4 mM could not be used due to low solubility. The amount of product increased until the enzyme concentration reached 2 μM, but slightly decreased at 4 μM compared to 2 μM of the enzyme (Figure 1C).

3.4. Effect of temperature and pH on BHET hydrolysis

Effects of temperature and pH on BHET hydrolysis by Cut190* were investigated. The enzyme activity increased as the temperature increased up to 60 ℃ (Figure 2A). The enzyme activity also slightly increased with increase in pH up to 8.5 (Figure 2B). Under the condition of 1 mM BHET in 1% DMSO, 50 mM Tris-HCl (pH 7.5), 5 or 25 mM $CaCl_2$ at 37 ℃, the time-course experiments showed that the progress curve was linear until 8 or 4 h, respectively (Figures 3A,B and S5A,B). In addition to Cut190*, Cut190*Q138A/D250C-E296C also showed linear progress until 2 h at 5 and 25 mM $CaCl_2$ (Figures 3C,D and S5C,D). To compare the activities of the two mutant enzymes towards BHET, the substrate conversion after 2 h was determined. The substrate conversion rates of Cut190* at 5 and 25 mM Ca^{2+} were 8.3% and 12.4%, respectively, and those of Cut190*Q138A/D250C-E296C were 20.8% and 21.7%, respectively.

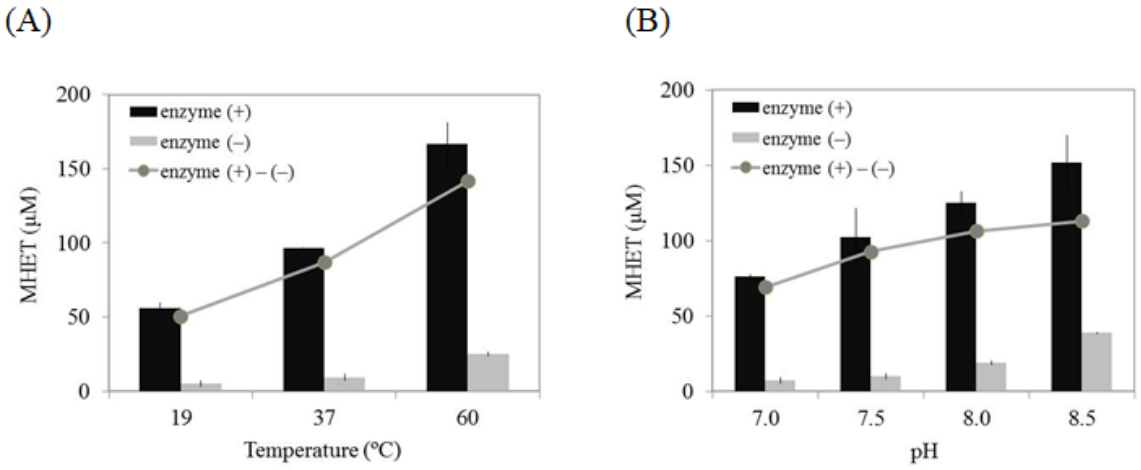

Figure 2. Effect of temperature (A) and pH (B) on Cut190* activity towards BHET. Black and grey bars were MHET amounts in the reaction mixtures with and without enzyme, respectively. Grey circles were MHET amounts subtracted without enzyme from with enzyme to indicate net enzyme activities. Data are shown with the standard deviation of triplicate measurements.

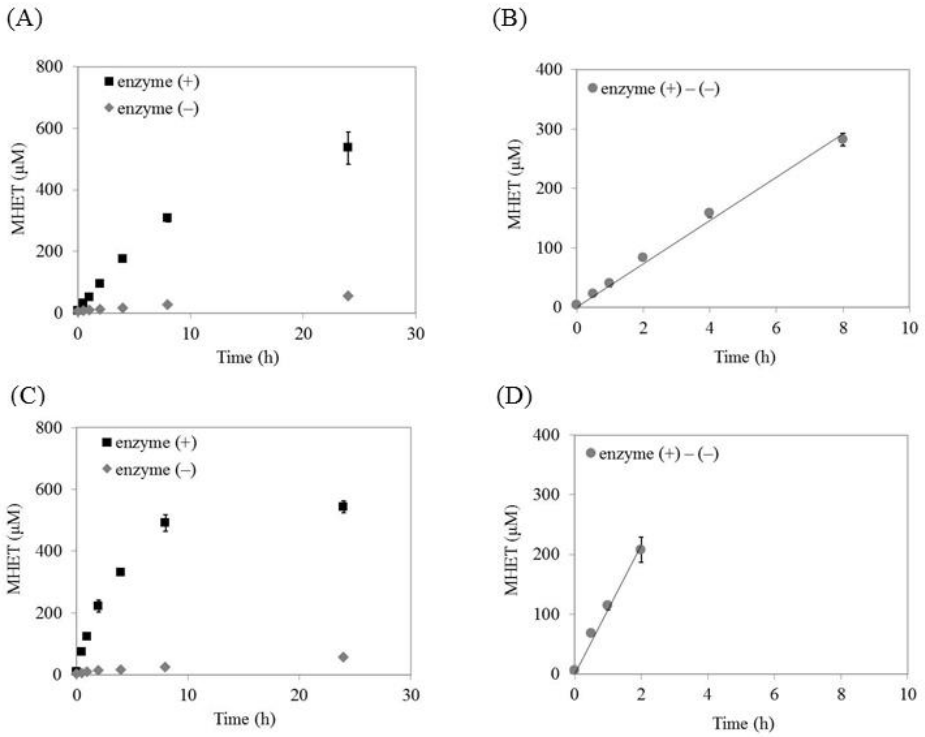

Figure 3. Time course of BHET hydrolysis by Cut190* (A, B) and Cut190*Q138A/D250C-E296C (C, D) in the presence of 5 mM Ca^{2+}. Black squares and grey diamonds in A and C were MHET amounts in the reaction mixtures with and without enzyme, respectively. Grey circles in B and D were MHET amounts subtracted without enzyme from with enzyme to indicate net enzyme activities. Data are shown with the standard deviation of triplicate measurements.

3.5. Effect of pressure on enzyme activity and structure

Activities of Cut190* and Cut190*Q138A/D250C-E296C in the presence of 5 or 25 mM $CaCl_2$ were measured under different pressures (up to 400 MPa). The results showed that the amounts of product depended on pressure, and the highest values were obtained at 400 MPa (Figure 4A). Hydrolysis of BHET was observed not only in the presence of enzyme, but also in the absence of enzyme. In order to compare the net enzyme activities, the MHET amount without the enzyme was subtracted from that obtained with enzyme. The results revealed that increase in enzyme activity due to pressurization was not observed. The enzyme activity in the presence of 5 mM Ca^{2+} was kept under high pressure of 400 MPa (Figure 4A,C). On the other hand, the enzyme activity at 25 mM Ca^{2+} tended to decrease under high pressure (Figure 4B,D).

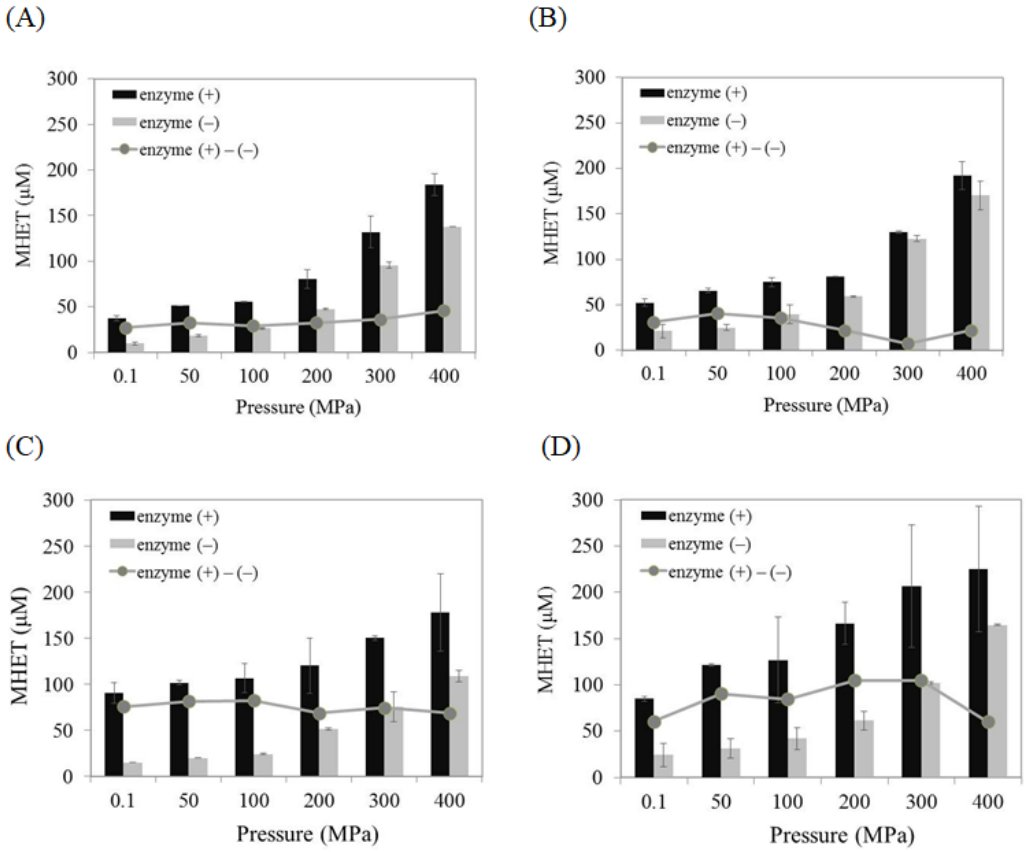

Figure 4. Effect of pressure on Cut190* activity towards BHET (A, B) and Cut190*Q138A/D250C-E296C (C, D) in the presence of 5 mM (A, C) or 25 mM Ca^{2+} (B, D). Black and grey bars were MHET amounts in the reaction mixtures with and without enzyme, respectively. Grey circles were MHET amounts subtracted without enzyme from with enzyme to indicate net enzyme activities. All data are shown with the standard deviation of triplicate measurements.

Effects of pressure on the secondary structure of Cut190* were analyzed using FTIR experiments. At relatively low pressures, the FTIR absorbance spectra of Cut190* showed a prominent peak at ~1638 cm^{-1} with shoulders at ~1652 cm^{-1} and ~1674 cm^{-1} (Figure 5A). Resolution enhancement by a second derivative analysis [19] indicated that there were peaks at 1629 cm^{-1}, 1638 cm^{-1}, 1654 cm^{-1}, and 1674 cm^{-1} in the spectra at relatively low pressures (Figure 5B) (note that a second derivative spectrum gives a negative peak). According to the empirical and theoretical rules in literature [20–23], it is probable that the peaks at 1629 cm^{-1}/1638 cm^{-1}, 1654 cm^{-1}, and 1674 cm^{-1} stem from β-sheets, α-helices, and β-sheets (or turns), respectively. This assignment is in line with the secondary structures in the crystal structure of the enzyme [6,9]. The second derivative spectra remained almost unchanged in the region of pressure < 300 MPa, suggesting that the secondary structures were preserved under these pressures. Indeed, pressure dependence of the second derivative spectral intensity at 1638 cm^{-1}, i.e., the β-sheets depicts that the onset of structural change was at ~400 MPa (Figure 5C). Figure 5C also suggested that the midpoint of the unfolding is ~730 MPa. Reaching a plateau of the unfolding curve required a pressure over 1000 MPa. The spectrum after

decompression was almost identical to those of the native structure at relatively low pressures (Figure 5B), indicating that the structural change induced by pressure was reversible.

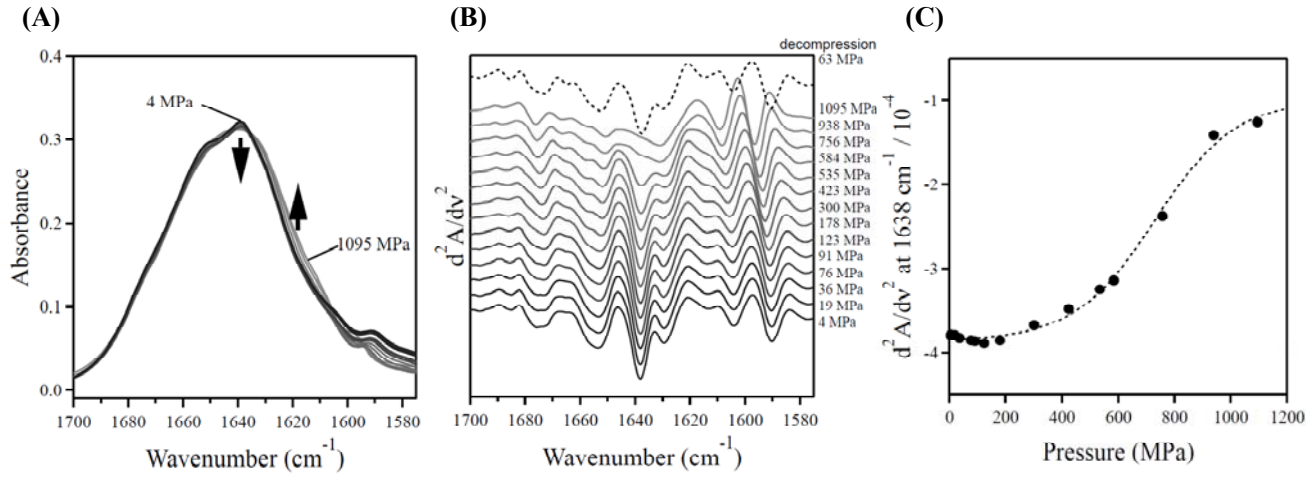

Figure 5. Effect of pressure on the structure of Cut190*. (A) Pressure dependence of FTIR spectra in the amide I' region of Cut190*. The spectra at higher pressures are shown as greyer colors. (B) Their second-derivative spectra. A dotted line indicates the spectrum after decompression. (C) Pressure dependence of the second derivative spectral intensity at 1638 cm^{-1}. A sigmoidal curve obtained by fitting the observed data (closed circle) is shown as the dotted line (for guiding the eyes).

4. Discussion

Due to high activity and thermal stability of Cut190*, it can be used in the industrial applications to hydrolyze PET. We previously analyzed the catalytic activity of Cut190* towards PBSA, pNPB and PET [4,7]; our results indicate that the mutant, Cut190*Q138A/D250C-E296C, exhibited higher activity and stability as compared to Cut190* [5]. In this study, we used BHET (the intermediate product of PET degradation (Figure S1)) as the model substrate for the activity analysis of Cut190* and Cut190*Q138A/D250C-E296C. The main product of the hydrolysis was MHET (Figure S2). Although TPA was supposed to be the final product (Figure S1), only the intermediate product, MHET, was generated, possibly due to the higher K_m of MHET than ~610 μM produced. The activity of Cut190* towards BHET was observed even in the absence of Ca^{2+} and increased with the increase in Ca^{2+} concentration (Figure 1A), which is similar to the activity towards pNPB but different from its activity towards PBSA; the activity is maximum under 2.5 mM Ca^{2+} [4,5]. This might be due to the size of substrate. Based on the crystal structure analysis of Cut190*S176A (inactive mutant of Cut190*) in complex with Ca^{2+} and the substrates [9], Ca^{2+} binding induced the enzyme "open" conformation in the enzyme and affected the shape of the catalytic site. The larger substrates such as PBSA could only bind to the enzyme in the "open" structure, while the smaller substrates such as pNPB and BHET could bind to the enzyme even in the "closed" structure. Under high Ca^{2+} concentrations, the molecular mechanism of Cut190* for the hydrolysis of BHET would be similar to that for the hydrolysis of pNPB, but different from that for the hydrolysis of PBSA. The increased

activity of Cut190* in pH up to 8.5 (Figure 2B) is similar to those for most of the cutinases from *Alternaria brassicicola* [24], *Thermobifida fusca* [25], *Fusarium solani* [26], and lipase from *Egyptian bacilli* [27] as well as Cut190* towards PBSA [4]. The increased activity in temperature up to 60 ℃ (Figure 2A) is similar to those for cutinases from thermophile *Thermobifida fusca* [25,28]. Considering that the thermal denaturation of Cut190*S176A in the presence of 2.5 mM Ca^{2+} starts around 60 ℃ and the transition temperature is 64.4 ℃ [8], around 60 ℃ would be the optimum temperature. This stability against pH and temperature is supposed to be advantageous for PET degradation, because PET is prone to chemical decomposition at high pH and temperature.

In addition to Cut190*, the catalytic activity of Cut190*Q138A/D250C-E296C towards BHET was evaluated. The k_{cat} values could not be determined due to the low solubility of BHET [29,30]. An analogue of BHET with high solubility will make it possible to determine the enzyme kinetics. The ratio of the substrate conversion indicated that the mutation Q138A together with the introduction of disulfide bond between the residues 250 and 296 could increase the activity, similar to the findings of studies on PBSA and PET-GF films [5]. Using the two mutants, we also analyzed the effect of pressure on the catalytic activity. With increasing pressure up to 400 MPa, the conversion rate of BHET into MHET gradually increased up to approximately 20% (Figure 4). Quartinello et al. recently reported that pressure (4 MPa) at high temperature (250 ℃) is effective in PET degradation [14]. To our knowledge, this is the first report of BHET degradation analysis at high pressures (~400 MPa), showing that high pressure even at low temperature (37 ℃) is effective in BHET degradation. Under all the conditions of high pressures analyzed, the activities of enzymes were remained, and the BHET conversion rate in the presence of enzyme was higher than that in the absence of enzyme. The FTIR experiments under high pressure indicated that Cut190* molecules with the native structure were still dominantly populated at 400 MPa (Figure 5). In the structural stability analysis against pressure in terms of the secondary structural change using FTIR, the loss of the β-sheets was used as an indicator of the folding-unfolding equilibrium (Figure 5C). This analysis indicated that most of the enzyme molecules were populated in the native structure below ~400 MPa. Thus, the loss of activity by pressure-induced unfolding would be negligible in the region of pressure. The midpoint of the Cut190* unfolding was determined to be ~730 MPa (Figure 5C), which is comparable to those of other globular proteins reported previously [31,32]. The reversibility of pressure-induced unfolding is contrary to the irreversibility of thermal denaturation [8]. There were minor spectral changes such as a red shift of the peak at ~1654 cm^{-1} even between 4 MPa and 300 MPa. This could be because high-pressure FTIR spectral changes involve an elastic effect including a change in strength of hydrogen bond in helices in addition to effect of a conformational change [16]. Under the conditions of high pressure where the enzyme activity is increased [10–12], high-pressure FTIR will be a powerful tool to evaluate the structure - activity relationship (SAR) of the enzyme. Taken together, as pressure increases, the structural flexibility of Cut190* might be unchanged or the increase might be smaller than the increase in the non-enzymatic degradation rate of BHET.

5. Conclusion

In conclusion, we showed that BHET could be used as a substitute for PBSA, pNPB, and PET for the analysis of Cut190* activity. The investigation for Ca^{2+} effect on the enzyme activity suggested that small size of substrate could bind to not only "open" form of Cut190* but also the "closed" form. We also found out the additive effects of enzyme and pressure (up to 400 MPa). The present

finding that hydrolysis of BHET even in the absence of enzyme increased with increase in pressure suggests the possibility of PET degradation by high pressure.

Acknowledgements

The authors thank Drs. Akihiro Maeno and Kazuyuki Akasaka for technical support of high-pressure experiments. This work was supported by Institute for Fermentation, Osaka (IFO).

Conflict of interest

All authors declare no conflict of interest in this paper.

References

1. Chen S, Su L, Chen J, et al. (2013) Cutinase: characteristics, preparation, and application. *Biotechnol Adv* 31: 1754–1767.
2. Wei R, Zimmermann W (2017) Biocatalysis as a green route for recycling the recalcitrant plastic polyethylene terephthalate. *Microb Biotechnol* 10: 1302–1307.
3. Zimmermann W, Billig S (2010) Enzymes for the biofunctionalization of poly(ethylene terephthalate). *Adv Biochem Eng Biotechnol* 125: 97–120.
4. Kawai F, Oda M, Tamashiro T, et al. (2014) A novel Ca^{2+}-activated, thermostabilized polyesterase capable of hydrolyzing polyethylene terephthalate from *Saccharomonospora viridis* AHK190. *Appl Microbiol Biotech* 98: 10053–10064.
5. Oda M, Yamagami Y, Oida I, et al. (2018) Enzymatic hydrolysis of PET: Functional roles of three Ca^{2+} ions bound to a cutinase-like enzyme, Cut190*, and its engineering for improved activity. *Appl Microbiol Biotech* 102: 10067–10077.
6. Miyakawa T, Mizushima H, Ohtsuka J, et al. (2015) Structural basis for the Ca^{2+}-enhanced thermostability and activity of PET-degrading cutinase from *Saccharomonospora viridis* AHK190. *Appl Microbiol Biotech* 99: 4297–4307.
7. Kawabata T, Oda M, Kawai F (2017) Mutational analysis of cutinase-like enzyme, Cut190, based on the 3D docking structure with model compounds of polyethylene terephthalate. *J Biosci Bioeng* 124: 28–35.
8. Inaba S, Kamiya N, Bekker GJ, et al. (2018) Folding thermodynamics of PET-hydrolyzing enzyme Cut190 depending on Ca^{2+} concentration. *J Therm Anal Calorim*.
9. Numoto N, Kamiya N, Bekker GJ, et al. (2018) Structural dynamics of the PET-degrading cutinase-like enzyme from *Saccharomonospora viridis* AHK190 in substrate-bound states elucidates the Ca^{2+} driven catalytic cycle. *Biochemistry* 57: 5289–5300.
10. Masson P, Tonello C, Balny C (2001) High-pressure biotechnology in medicine and pharmaceutical science. *J Biomed Biotechnol* 1: 85–88.
11. Buckow R, Weiss U, Heinz V, et al. (2007) Stability and catalytic activity of -amylase from barley malt at different pressure-temperature conditions. *Biotechnol Bioeng* 97: 1–11.
12. Eisenmenger MJ, Reyes-De-Corcuera JI (2009) High pressure enhancement of enzymes: A review. *Enzyme Microb Technol* 45: 331–347.

13. Bamdad F, Bark S, Kwon CH, et al. (2017) Anti-inflammatory and antioxidant properties of peptides released from β-lactoglobulin by high hydrostatic pressure-assisted enzymatic hydrolysis. *Molecules* 22: E949.
14. Quartinello F, Vajnhandl S, Volmajer Valh J, et al. (2017) Synergistic chemo-enzymatic hydrolysis of poly(ethylene terephthalate) from textile waste. *Microb Biotechnol* 10: 1376–1383.
15. Yamanis J, Vilenchich R, Adelman M (1975) Gas-liquid chromatography of silylated glycols and terephthalate esters. *J Chromatogr A* 108: 79–84.
16. Dzwolak W, Kato M, Taniguchi Y (2002) Fourier transform infrared spectroscopy in high-pressure studies on proteins. *Biochim Biophys Acta* 1595: 131–144.
17. Imamura H, Isogai Y, Kato M (2012) Differences in the structural stability and cooperativity between monomeric variants of natural and de novo Cro proteins revealed by high-pressure Fourier transform infrared spectroscopy. *Biochemistry* 51: 3539–3546.
18. Wong PTT, Moffatt D (1989) A new internal pressure calibrant for high-pressure infrared spectroscopy of aqueous systems. *Appl Spectrosc* 43: 1279–1281.
19. Savitzky A, Golay MJE (1964) Smoothing and differentiation of data by simplified least squares procedures. *Anal Chem* 36: 1627–1639.
20. Barth A, Zscherp C (2002) What vibrations tell us about proteins. *Q Rev Biophys* 35: 369–430.
21. Byler DM, Susi H (1986) Examination of the secondary structure of proteins by deconvolved FTIR spectra. *Biopolymers* 25: 469–487.
22. Torii H, Tasumi M (1992) Model calculations on the amide-I infrared bands of globular proteins. *J Chem Phys* 96: 3379–3387.
23. Ganim Z, Chung HS, Smith AW, et al. (2008) Amide I two-dimensional infrared spectroscopy of proteins. *Acc Chem Res* 41: 432–441.
24. Koschorreck K, Liu D, Kazenwadel C, et al. (2010) Heterologous expression, characterization and site-directed mutagenesis of cutinase $CUTAB_1$ from *Alternaria brassicicola*. *Appl Microbiol Biotechnol* 87: 991–997.
25. Chen S, Tong X, Woodard RW, et al. (2008) Identification and characterization of bacterial cutinase. *J Biol Chem* 283: 25854–25862.
26. Kwon MA, Kim HS, Yang TH, et al. (2009) High-level expression and characterization of *Fusarium solani* cutinase in *Pichia pastoris*. *Protein Expression Purif* 68: 104–109.
27. Kim HR, Song WS (2010) Optimization of papain treatment for improving the hydrophilicity of polyester fabrics. *Fibers Polym* 11: 67–71.
28. Billig S, Oeser T, Birkemeyer C, et al. (2010) Hydrolysis of cyclic poly(ethylene terephthalate) trimers by a carboxylesterase from *Thermobifida fusca* KW3. *Appl Microbiol Biotechnol* 87: 1753–1764.
29. Barth M, Oeser T, Wei R, et al. (2015) Effect of hydrolysis products on the enzymatic degradation of polyethylene terephthalate nanoparticles by a polyester hydrolase from *Thermobifida fusca*. *Biochem Eng J* 93: 222–228.
30. Joo S, Cho IJ, Seo H, et al. (2018) Structural insight into molecular mechanism of poly(ethylene terephthalate) degradation. *Nat Commun* 9: 382.
31. Gall A, Ellervee A, Sturgis JN, et al. (2003) Membrane protein stability: high pressure effects on the structure and chromophore-binding properties of the light-harvesting complex LH2. *Biochemistry* 42: 13019–13026.

32. Dirix C, Duvetter T, Loey AV, et al. (2005) The *in situ* observation of the temperature and pressure stability of recombinant *Aspergillus aculeatus* pectin methylesterase with Fourier transform IR spectroscopy reveals an unusual pressure stability of β-helices. *Biochem J* 392: 565–571.